J. Membrane Biol. 46, 71–89 (1979)

Capacitance and Conductance as Tools for the Measurement of Asymmetric Surface Potentials and Energy Barriers of Lipid Bilayer Membranes

Peter Schoch, David F. Sargent, and Robert Schwyzer

Institut für Molekularbiologie und Biophysik, Eidgenössische Technische Hochschule, CH-8093 Zürich, Switzerland

Received 13 September 1978; revised 28 November 1978

Summary. A simple method for the determination of asymmetric surface potentials in lipid bilayers is described. The method is based on the dependence of bilayer capacitance on transmembrane voltage. The capacitance is measured by rectifying the 90° component of an applied alternating current signal. A superimposed slow triangular wave results in a hysteresis-like time course of capacitance. The center of the hysteresis figure is shifted along the voltage axis by an amount equal to the difference of the dipole plus surface-charge potentials on the two sides of the bilayer (capacitance minimization potential).

Alternatively, such bilayer asymmetry was studied by using the current-voltage characteristics in the presence of nonactin as a carrier. This analysis was based on the integrated Nernst-Planck equation, assuming a trapezoidal energy barrier and equilibrium of the surface reactions.

The two methods gave consistent results for the surface potentials of phosphatidyl serine membranes asymmetrically shielded with calcium. In addition, the current analysis yields the positions of the corners of the barrier, found to be set in 13 % for this lipid.

It is becoming more and more evident that a great many membrane-dependent biological processes are influenced by electric fields. Artificial planar membranes are a widely used model system in membrane studies. The present paper deals with two methods for measuring the electrostatic potentials at the bilayer-solution interface.

From a biological point of view two parameters of the electrostatic potential energy barrier associated with membranes are of main interest: (i) the potential gradient inside the membrane, which affects the activity of intrinsic membrane proteins, and (ii) the potential difference between the bulk electrolyte solution and the membrane surface, which influences membrane fusion and the interaction of the membrane with soluble

0022-2631/79/0046-0071 $03.80

molecules. Both these quantities are greatly dependent on the lipid composition of biological membranes.

For the evaluation of the electrostatic potential energy barrier we developed a new method, based on voltage-dependent membrane capacitance, to measure the potential gradient within the bilayer (Schoch & Sargent, 1976). In this paper we give a detailed justification of the method through comparison with the surface potentials calculated from the analysis of current-voltage curves using nonactin-K^+ as the permeant species. The results are also compared with the predictions of the Gouy-Chapman theory.

Theory

Electrostatic Potential Energy Barrier

The electrostatic potential at the membrane-solution interface is composed of several components (*see*, for example, Aveyard & Haydon, 1973, Haydon, 1975, or McLaughlin, 1977). Figure 1*a* summarizes the situation. In the case of charged lipid molecules there is a diffuse ionic double-layer potential originating from a fixed-charge layer in combination with the adjacent aqueous electrolyte solution. Its maximal value relative to the bulk solution, V_G, lies just at the interface. In the polar head group region there is a further potential jump, V_D, resulting either from the molecular dipoles of the lipids themselves or from oriented water molecules.

These two components, V_G and V_D, or more exactly the fields associated with them, are the ones influencing the voltage-dependent capacitance. The result of summing the two potentials is presented schematically in Fig. 1*b*. The difference in the heights of the two corners at zero applied voltage, $\Delta\Psi$, is equal to the difference of the surface potentials of the two sides of the bilayer.

$$\Delta\Psi = \Delta V_G + \Delta V_D. \tag{1}$$

$\Delta\Psi$ is therefore a measure of the asymmetry of the electrostatic potentials associated with the membrane and is the parameter that is determined by our method of voltage-dependent membrane capacitance.

For the analysis of current-voltage curves there is a third component to take into account, namely, the Born self-energy of a charge in the low dielectric medium of the membrane. This self-energy, V_B, is smoothed near the interface by interaction with induced dipoles; mathematically it

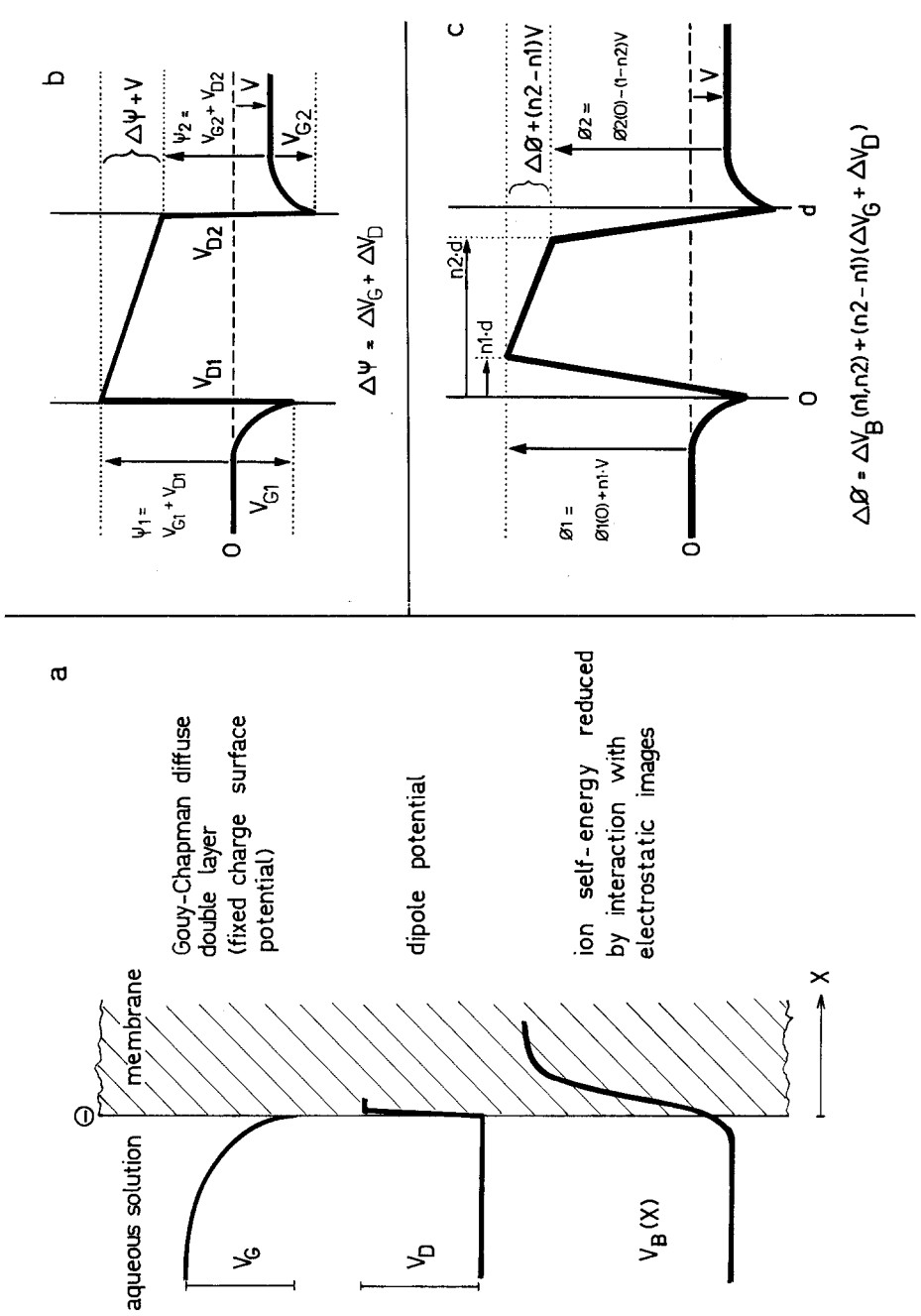

Fig. 1. Schematic representation of electrostatic potentials at the membrane-solution interfaces. (*a*): Individual components. In addition to the surface potentials V_G and V_D, ions crossing the membrane experience the so-called Born-potential, V_B, which depends on the size and the dielectric surroundings of the ion. (*b*): The sum of the surface potentials adjacent to a bilayer membrane, resulting in an intrinsic field $\Delta\Psi/d$ even without an externally applied voltage V. $\Delta\Psi$ is measured as the externally applied potential for minimal membrane capacitance. (*c*): The trapezoidal energy barrier for ions crossing a lipid membrane. $\Delta\Phi$ gives the asymmetry of the barrier at zero applied voltage and determines, together with the positions of the two corners ($n1$ and $n2$), the shape of the current-voltage curve

is treated as an interaction of the charge with its "electrostatic images" (Neumcke & Läuger, 1969, Parsegian, 1975).

The total energy barrier takes on the trapezoidal shape shown schematically in Fig. 1*c*. Because V_B is strongly reduced near the interface by attraction of the charge to its image, the corners of the barrier are displaced significantly toward the center of the membrane. Their positions 1, $n1$ and $n2$, are given formally as fractions of the membrane thickness, d. The parameter that reflects the potential difference across the membrane and that appears in the current-voltage relation is called $\Delta\Phi$. It is defined as the difference in the heights of the two corners at zero applied voltage:

$$\Delta\Phi = \Delta V_B(n1, n2) + (n2 - n1)(\Delta V_G + \Delta V_D). \tag{2}$$

Two special cases of particular interest of the general equations (1) and (2) may be distinguished, depending on the membrane-electrolyte system chosen. (i) Symmetrical, charged lipid membrane, different shielding electrolyte solutions: $\Delta V_G \neq 0$, $\Delta V_D = 0$, and $\Delta V_B = 0$. The latter two conditions stem from the dielectric symmetry of the membrane. Equations (1) and (2) now reduce to

$$\Delta\Psi = \Delta V_G \tag{3a}$$

and

$$\Delta\Phi = (n2 - n1)\,\Delta V_G. \tag{3b}$$

This is the case considered in the experiments reported here. (ii) Asymmetrical, but neutral, lipid membrane: $\Delta V_G = 0$ and $\Delta V_D \neq 0$. Such systems will be described in a future paper.

Capacitance-Voltage Characteristic

Several investigators have demonstrated that solvent-containing lipid bilayers show a voltage-dependent capacitance, $C_m(V)$. To our knowledge, Babakov, Ermishkin and Liberman (1966) were the first to note that C_m increases with the square of the applied voltage, and later White (1970) reported an extensive study of the effect. This voltage dependence is explained by geometric changes brought about by electrocompression, which results mainly in a decrease of membrane thickness by a squeezing out of hydrocarbon solvent into microlenses and the torus at approximately constant area. As we pointed out earlier (Schoch & Sargent,

1976), the field acting on the bilayer is composed of two components – the externally applied field, V, and an intrinsic field due to any difference in surface potential on the two sides of the bilayer, $\Delta\Psi$. The effects of electrocompression may therefore be described by

$$\frac{C_m(V)-C_0}{C_0}=\frac{\Delta C_m}{C_0}=\beta(\Delta\Psi+V)^2 \tag{4}$$

where C_0 is the *minimal* capacitance, $C_m(V)$ is the voltage-dependent capacitance, β is a proportionality factor, V is the applied voltage, and $\Delta\Psi$ is the difference of the surface potentials. The formula shows that for any asymmetry in surface potentials ($\Delta\Psi\neq 0$) there exists an applied voltage, V, such that $\Delta C_m=0$. The voltage that satisfies this condition is called here the "capacitance minimization potential":

$$V_{C\min}=-\Delta\Psi. \tag{5}$$

In the special case of symmetrical, charged lipid bilayers but different shielding electrolytes, as in the experiments reported here, Eqs. (5) and (3*a*) reduce to:

$$V_{C\min}=-\Delta V_G. \tag{6}$$

Current-Voltage Characteristics

Many theoretical derivations of equations describing transport of ions by neutral carriers have been published in the last few years (Haydon & Hladky, 1972; Hladky, 1972; Läuger & Neumcke, 1973; Ciani et al., 1973). Whereas the general expressions are very complex, it's often possible to formulate simpler ones by making reasonable assumptions. For example, with nonactin the interfacial reactions are fast compared with the actual translocation step across the membrane, as indicated by the experimentally observed superlinear current-voltage characteristic (e.g., Fig. 3) (Läuger & Stark, 1970; Stark & Benz, 1971). The rate constants determined by Hladky (1975) confirm that the rate-limiting step is indeed the translocation through the interior of the membrane ($k_{is}/k_{Di}\ll 1$). In the same paper Hladky showed that the steady-state current is attained in the μsec region, so that our current-voltage curves recorded at a sweep rate of 100 mV/sec are effectively

steady-state values. Further, by checking the effect of stirring we could show that there was no diffusion limitation in the aqueous phases: the phenomenon described by Hladky (1973), found when nonactin is added to the aqueous phases, was seen, but there was no change of the basic *shape* of the current-voltage curve.

Given that the surface reactions are in approximate equilibrium, we may ignore the fine structure of the potential near the interface and consider the situation shown in Fig. 1*c*. Such a barrier shape was derived by Hall, Mead & Szabo (1973) by examining experimental current-voltage curves. For our calculations, we postulate a Boltzmann distribution of the permeant ions between the bulk solution and the corners of the membrane energy barrier. By using the constant field approximation, the current across the membrane, I_m, may be calculated by application of the Nernst-Planck flux equation, as indicated in the *Appendix*. The result is:

$$I_m = K \frac{(\Delta\Phi + (n2 - n1)\,V)}{n2 - n1} \frac{e^{aV} - 1}{e^{a(\Delta\Phi + n2 \cdot V)} - e^{an1 \cdot V}} \tag{7}$$

where K is a constant factor for each individual membrane, a has the value of 1/25.4 mV at room temperature, and $n1$, $n2$ and $\Delta\Phi$ describe the trapezoidal barrier (*see* Fig. 1*c*). V is the applied voltage. A similar equation was derived by Hladky (1974); however, no allowance was made there for membrane asymmetry ($n1 \neq 1 - n2$, unequal surface potentials).

Materials and Methods

Membrane Formation and Electrolyte Solutions

Lipid bilayer membranes were formed essentially by the technique of Montal and Mueller (1972): two separately formed monolayers are apposed over an aperture in a thin septum. The measurement of voltage-dependent capacitance is easier if the "monolayers" still contain some solvent, resulting in greater compressibility.

The lipid used was the monosodium salt of bovine phosphatidyl serine (grade I, Lipid Products, South Nutfield, Surrey, England) dissolved at 0.7 % in hexane.

The bilayer was formed on a thin Teflon septum 30 μm thick (Beckman Instruments, No. 77948-D) into which a small hole of about 0.06–0.08 mm^2 area was melted by a glowing filament. The orifice was not pretreated before membrane formation. The Teflon septum was clamped between two half-cells, each containing 5 ml of an aqueous electrolyte solution. The electrolyte was usually 0.01 M KCl buffered by 2 mM imidazole (pH 7.0) and contained 5×10^{-7} M nonactin (Sigma) as required. To get asymmetric

electrolyte solutions, 50 μl amounts of concentrated $CaCl_2$ solutions were added to one chamber to get the appropriate Ca^{2+} concentrations in the range of 10^{-6} to 10^{-3} M. All experiments were performed at 22 ± 1 °C.

Experimental Set-up

A block diagram of the experimental set-up is shown in Fig. 2. The whole assembly was developed and built in this laboratory. The Ag/AgCl reference electrodes (Ingold, Switzerland) are connected to the measurement chambers by agar/salt bridges. The salt bridges have a resistance of about $1 k\Omega$ each and are the limiting resistance of the circuit.

Current was measured with a Teledyne-Philbrick 1027 operational amplifier connected as a current-voltage converter (10^7 V/A) followed by an amplifier with variable gain (1 to 1000). For a convenient, continuous monitoring of the bilayer *capacitance*, the 90° component of the 1000-Hz current signal was rectified and normalized with the amplitude of the applied ac voltage.

The *voltmeter* is a high impedance, low offset device based on the Burr-Brown 3523L operational amplifier.

The *function generator* allows the generation of dc-offsets, sine waves of 10 to 10^4 Hz, pulses of variable heights and lengths, and ramps with selectable endpoints and slopes (0.2 mV/sec to 10 V/sec). The various signals are mixed and applied to the membrane via a variable series resistor. The membrane simulating device (5 kΩ potentiometer in series with a parallel variable *R-C* combination) with accurate, calibrated elements, served in the present experiments only for adjusting the capacitance-measuring circuit.

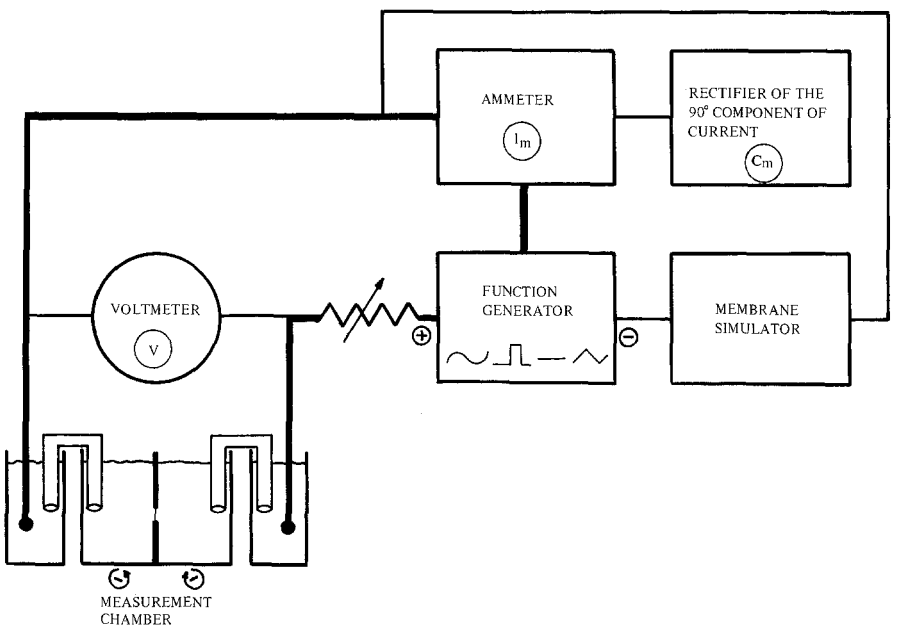

Fig. 2. Block diagram of the experimental set-up. For the description of each element *see Materials and Methods*

Results

Capacitance-Voltage Curves

Figure 3 shows a representative measurement of the current and capacitance characteristics of a phosphatidyl serine membrane. Figure 3*a* was recorded with no added calcium, while in Figure 3*b* the negative lipid surface charges are shielded on one side by 1.1×10^{-5} M Ca^{2+}. The capacitance versus voltage curves in the upper parts of the figures were recorded at a sweep rate of 100 mV/sec. The adaptation of the membrane capacitance to the applied voltage extends over the msec to sec range,

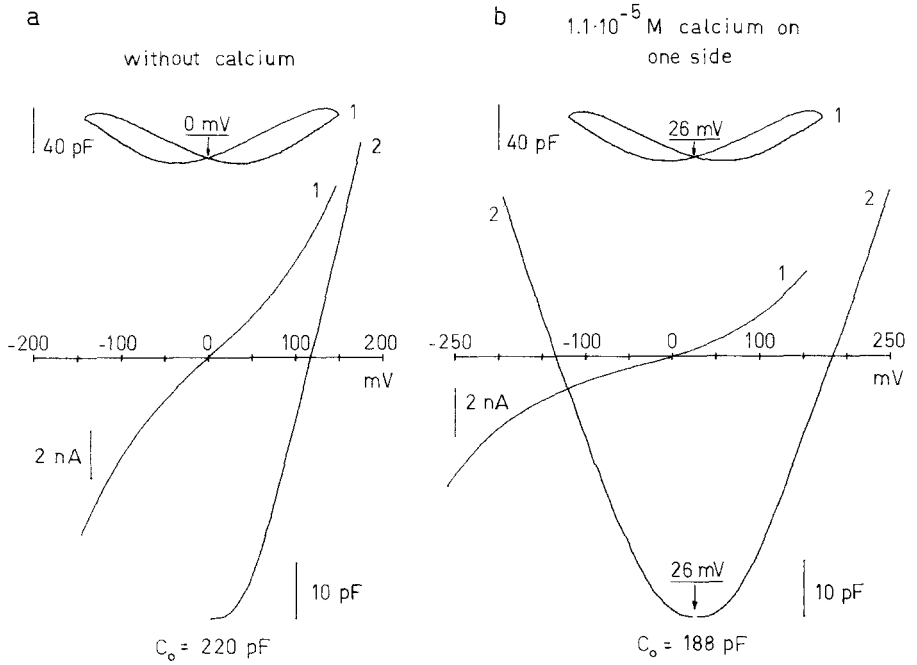

Fig. 3. Representative measurements of the current and capacitance characteristics of a PS membrane. The bilayer has a rather high hexane content to emphasize the capacitance response. Electrolyte: 0.01 M KCl, 2 mM imidazole, pH 7.0, plus 5×10^{-7} M nonactin. (*a*): without calcium. (*b*): 1.1×10^{-5} M $CaCl_2$ added to the side connected to the ammeter (side 1). Membrane area was $\simeq 6 \times 10^{-2}$ mm^2. The continuous capacitance *vs.* voltage curves are shown at the top of the figure. In *b* the asymmetrical addition of Ca^{2+} has caused the center of the hysteresis-like curve to be shifted to 26 mV. This shift is called the capacitance minimization potential, $V_{C\min}$. The bottom curves show the expanded capacitance characteristics, starting at the minimization potential and recorded with a slower sweep rate. The mid-sections give the appropriate current-voltage curves, showing the change caused by the added calcium. Curves labelled 1 were recorded at 100 mV/sec, those labelled 2 at 50 mV/sec

and may be different for increasing and decreasing voltages. This leads to a hysteresis-like capacitance sweep. The expanded capacitance curves in the lower parts of the figure show that the capacitance minima coincide with the centers of the hysteresis-like figures. Figure 3*b* shows that the minimum of the capacitance is shifted by 26 mV. This means that the intrinsic compression of the membrane, caused by the asymmetric surface potentials (ΔV_G in this case), is compensated at an externally applied voltage of 26 mV.

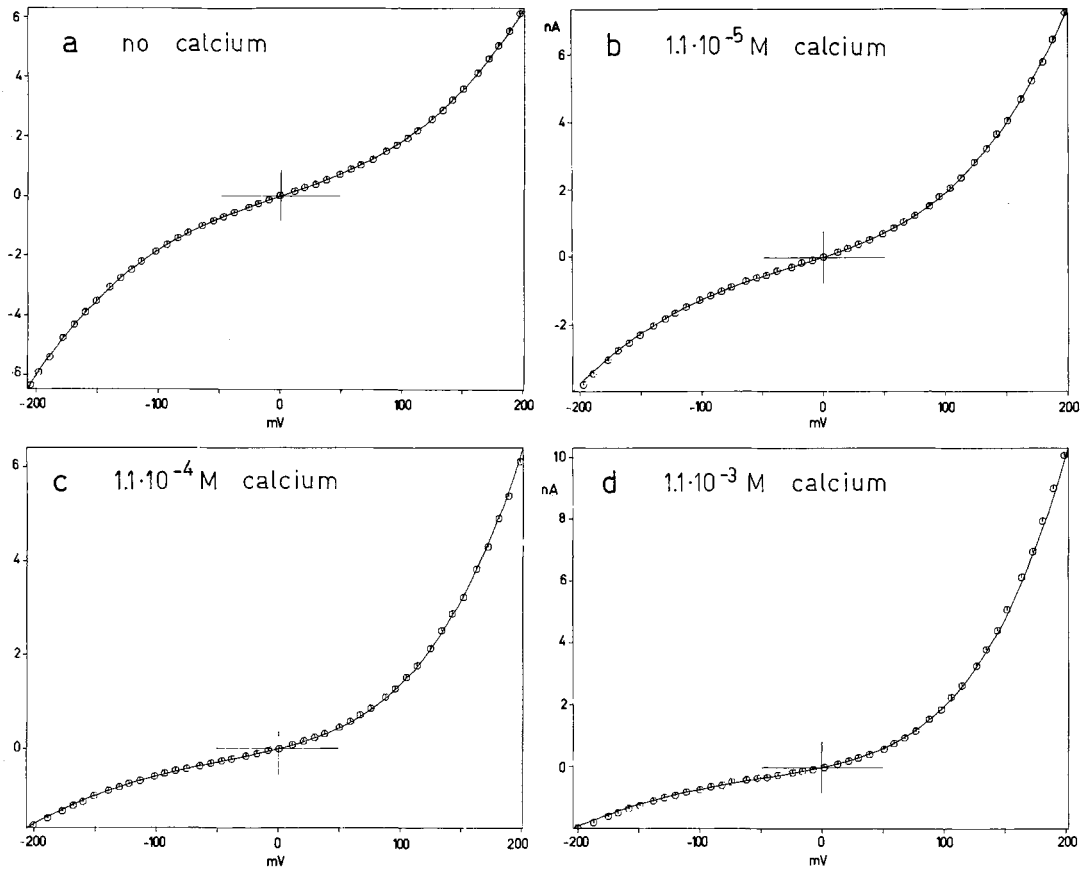

Fig. 4. Experimental current-voltage curves (points) fitted to Eq. (7) (solid line). The experiment represents a single PS membrane with various amounts of $CaCl_2$ added asymmetrically, as specified in the figures. Other experimental data are as indicated in the Table. The fitted parameters are: (*a*) $n1=0.14$, $n2=0.86$, $\Delta\Phi=1.6$ mV, $K=1.05\times10^{-2}$ nA/mV; (*b*) $\Delta\Phi=-27$ mV, $K=5.26\times10^{-3}$ nA/mV; (*c*) $\Delta\Phi=-55$ mV, $K=1.92\times10^{-3}$ nA/mV; and (*d*) $\Delta\Phi=-63$ mV, $K=2.25\times10^{-3}$ nA/mV. For *b*, *c* and *d*, *n*1 and *n*2 were held constant at the values found for curve *a*

Table. Summary of numerical results[a]

Ca^{2+} (M)	$-\Delta V_G = V_{C\min}$ (mV)	$n1=(1-n2)$	$-\Delta\Phi$ (mV)	$-\Delta V_G = \Delta\Phi/(n2-n1)$ (mV)	K[b] (nA/mV)
none	0 ± 2	0.13 ± 0.02	0 ± 2	0 ± 3	1.05×10^{-2}
1.0×10^{-6}	6 ± 2	0.13 ± 0.02	8 ± 4	10 ± 5	8.06×10^{-3}
1.1×10^{-5}	26 ± 3	0.13 ± 0.02	25 ± 6	34 ± 8	5.26×10^{-3}
1.1×10^{-4}	52 ± 3	0.13 ± 0.02	55 ± 6	74 ± 8	1.92×10^{-3}
1.1×10^{-3}	75 ± 6	0.13 ± 0.02	61 ± 8	82 ± 11	2.25×10^{-3}

[a] Experimental data: phosphatidyl serine membranes, 0.01 M KCl, 2 mM imidazole, pH 7.0, 5×10^{-7} M nonactin, $T=22\,°C$. Membrane area: $\sim8\times10^{-2}$ mm^2 (hole area), $C_0\simeq420$ pF (0.53 μF/cm^2).

The uncertainties are the standard deviations of the means.

[b] Values derived for one representative membrane only.

Current-Voltage Curves

The current-voltage curves for the two membranes are found in the mid-sections of Fig. 3. The parameters $\Delta\Phi$, $n1$ and $n2$ were extracted from the experimental curves by computer-fitting to Eq. (7) (James & Roos, 1975), or by superposition on computer-generated families of curves with systematically varied values of $\Delta\Phi$, $n1$ and $n2$. The results of such analyses are shown in Fig. 4.

The ΔV_G values derived from the analysis of the current-voltage curves and the $V_{C\min}$ values from the capacitance measurements are given in the Table.

Discussion

Voltage-Dependent Capacitance

In this report we have presented the details of a recently developed method to determine asymmetric electrostatic potentials in artificial lipid membranes. The method makes use of the fact that electric fields induce geometrical changes in the bilayers, sometimes called electrocompression or electrostriction, resulting in a voltage-dependent membrane capacitance, $C_m(V)$. In the last few years various authors have studied this effect. The amplitude of the changes depends strongly on the lipid used and on the type and content of hydrocarbon solvent (Benz & Janko, 1976). Several processes seem to be responsible for the phenomenon and could include:

a) An elastic compression resulting in a capacitance change of about 0.02 to 0.06 % at 100 mV. This adaptation exists in both solvent-free and solvent-containing membranes (Alvarez & Latorre, 1978; Wobschall, 1972).

b) An extrusion of solvent into microlenses and the border, resulting in a thinning of the membrane and a capacitance change of up to 10 % at 100 mV.

c) A creation of new membrane at the expense of the plateau border. The amplitude of this effect is thought to be small (<1 % at 100 mV), at least for membranes with a small torus/bilayer ratio.

d) A further slow increase, probably resulting from a reduction of the area occupied by the microlenses through fusion and coalescence with the border, and from the creation of new membrane in the case of big torus/bilayer ratios (Benz & Janko, 1976). These processes are only partially reversible.

The time scales of the various processes span a large range: *a* takes place within a few μsec, *b* and *c* occur in the msec to sec range (Raquena, Haydon & Hladky, 1975; Benz *et al.*, 1975, and our own observations), and process *d* takes even longer.

Mechanisms *a* and *b* have been found to accurately obey Eq. (4). For solvent-free PE[1] membranes, Alvarez and Latorre (1978) determined a β of $0.02\,V^{-2}$, while for solvent-containing bilayers β lies in the range of 2 to $10\,V^{-2}$ (White, 1970; White & Thompson, 1973; Benz *et al.*, 1975; Benz & Janko, 1976).

We were able to simulate the hysteresis-like $C_m(V,t)$ curves of Fig. 3 by assuming three first-order relaxation processes:

$$\tau_i^{\pm} \cdot \dot{C}_i + C_i = \beta_i \cdot V^2 \tag{8}$$

where C_i is the instantaneous capacitance of the ith relaxation component, $\tau_i^{\pm}$ are the time constants of the ith component for increasing and decreasing capacitance, respectively, and β_i is the relaxation amplitude of the ith component at 1 V. $\dot{C}_i$ represents the first time derivative of C_i.

For the membranes employed in this study the following values were derived: $\beta_1 \simeq \beta_2 \simeq 2$ to $5\,V^{-2}$, $\tau_1^+ = \tau_1^- \simeq 5$ msec, $\tau_2^+ \simeq 0.4$ sec, $\tau_2^- \simeq 0.6$ sec, $\beta_3 \simeq 1$ to $3\,V^{-2}$, $\tau_3^+ = \tau_3^- \simeq 5$ sec. At the 100 mV/sec sweep speed used, the fast relaxation is responsible for the overall "U" shape and the middle

[1] *Abbreviations used:* GDO, glycerol dioleate; PE, phosphatidyl ethanolamine; PS, phosphatidyl serine.

one for the "hysteresis". The slow component raises the whole figure on the C_m axis.

While sweeping more or less symmetrically around $V_{C\min}$ in the pseudo steady-state condition (retraceable $C-V$ curves), the center of the hysteresis-like figure indicates the voltage of minimal capacitance. Best resolution (i.e., highest slope at the crossing point) is found when the condition $f \cdot \tau_i = 1$ (f is the frequency of the triangular wave sweep) is satisfied for one of the relaxation components. Other factors being equal, the resolution increases with β_i and with sweep amplitude.

The idea that not only externally applied voltages but also intrinsic electrical fields resulting from asymmetric surface potentials might affect bilayer capacitance was suggested for the first time by Wobshall (1972). In 1976 we showed that this was indeed the case and applied the effect for the determination of surface potentials of asymmetric bilayers (Schoch & Sargent, 1976). More recently Alvarez and Latorre (1978) also used electrocompression in an analysis of surface potentials. They superimposed a 10-mV pulse on an arbitrary holding potential and used the integrated charging current as a measure of the capacitance. By measuring only the difference in charging currents for the bilayer and a matched $R-C$ network and using signal averaging techniques, they achieved high sensitivity, measuring a β of only $0.02\,V^{-2}$ in solvent-free bilayers. With our simple measuring technique we can study capacitance changes having a characteristic time constant of at least 4 msec and a magnitude of about 0.5 pF ($\simeq 0.1\,\%$) (the baseline capacitance is compensated by a bucking voltage circuit). This sensitivity allows the direct determination of β's of about $0.1\,V^{-2}$. An analysis of the surface potentials of solvent-free bilayers would also be possible by applying signal-averaging techniques and/or by measuring at a much shorter time scale in order to minimize the effects of slow drifts of membrane capacitance.

For the purpose of our work – the quantitative evaluation of surface potentials which arise in the polar head group region – the amount of hydrocarbon solvent contained in the bilayer seems to be immaterial, as we have shown in two studies. In the first, using egg lecithin membranes to which UO_2^{2+} was bound asymmetrically (Schoch & Sargent, 1976), no significant correlation was found between $V_{C\min}$ and β. From 20 membranes with β's ranging from 2 to $40\,V^{-2}$ we fitted the normalized $V_{C\min}$ and β to the following relation:

$$V_{C\min}/\bar{V}_{C\min} = a + b \cdot \beta. \tag{9}$$

The regression analysis yielded $b = 0.0008 \pm 0.0025$, showing that this

regression coefficient is not significantly different from zero. The same solvent-independent response was seen with hexane-containing phosphatidyl serine membranes made from monolayers ($\beta=1$ to $20\,V^{-2}$) in the presence of asymmetric shielding with $CaCl_2$. These findings are not unexpected in light of the fact that the area per lipid molecule seems to be independent of the solvent content, which influences only the thickness of the membranes (Fettiplace, Andrews & Haydon, 1971; Benz & Gisin, 1978).

Current-Voltage Characteristics

Other authors have also used nonactin-K^+ complexes as ionic probes for the determination of energy profiles in phospholipid bilayers. For PE membranes, the analysis by Krasne and Eisenman (1976) yields $n1=0.14$, whereas that by Hladky (1974) yields $n1=0.2$. The source of the discrepancy is not clear, but in this context it's important to note that electrostriction tends to increase the current, thereby leading to an overestimation of $n1$. Hall, Mead and Szabo (1973), Hall and Latorre (1976), and Latorre and Hall (1976) gave values of $n1$ between 0.28 and 0.32 for PE/PE, PS/PE and GDO/PE membranes. In our opinion these values are too high, presumably due to the fact that their analyses were based on a different voltage dependence, namely $I\alpha\exp(V/RT)$, as opposed to $I\alpha V\exp(V/RT)$, as derived in this and other papers (e.g., Hladky, 1974).

From computer-fitted values of K in Eq. (7) one may estimate the absolute height of the energy barrier relative to the bulk solution, $\Phi 1(0)$. By substituting $D=d^2 k_{is}/2$ into Eq. (A5), where k_{is} is the rate constant of the translocation step, the constant K becomes explicitly

$$K=zFAadk_{is}c_i c_s \gamma_s K_a \exp(-a\Phi 1(0))/2. \tag{10}$$

In evaluating $\Phi 1(0)$, we take the following numerical values: $d=35$ Å, $k_{is}=2\times 10^4\,sec^{-1}$ (Hladky, 1975), $\gamma_s=5000$ (cited in Hladky, 1974), $K_a=3.9\times 10^3$ 1/M. The latter value was measured in methanol by Wipf *et al.* 1968): as the transition of K^+ from water to methanol involves very little change in free energy (Strehlow, 1966), this value should also hold approximately for water.

Using $K=1.05\times 10^{-2}$ nA/mV (Table, line 1), one finds $\Phi 1(0)\simeq 300$ mV, which is quite satisfactory, considering the approximation made in the calculation.

Comparison of the Methods

Do the two methods, the $C(V)$ and $I(V)$ characteristics, give the same results? Although the corresponding values given in the Table differ significantly in only one case (1.1×10^{-4} M Ca^{2+}), the results from the current-voltage curves tend to yield ΔV_G values that are higher than those from the capacitance minimization method. We propose that the difference may arise from the nonideality of the membrane, as the diffusion coefficient, D, the membrane thickness, d, and the fractional distances $n1$ and $n2$ all depend on thickness and therefore voltage, in contrast to the conditions assumed in the derivation of Eq. (7). We have been able to derive a semi-empirical "error function", with only the instantaneous $C(V)$ as variable, that adjusts the experimental $I-V$ curves to the ones expected with rigid, voltage-independent parameters. This correction leads to better agreement between the two procedures for the evaluation of ΔV_G. Additionally it reveals that the nonideal voltage dependence affects the $I-V$ curves only when $|V-V_{C\min}|>150$ mV. It is therefore possible to interpret the $I-V$ curves over a limited range of voltage and get reasonable values for $\Delta\Phi$ even with compressible membranes. Details of this semi-empirical correction will be published elsewhere.

The Surface Charge Density of Phosphatidyl Serine Membranes

The electrostatic potential at the surface of a fixed charge sheet and in the diffuse double layer relative to the bulk solution has been shown to be adequately described at low electrolyte concentrations by the Gouy-Chapman theory (Aveyard & Haydon, 1973). Our results are consistent with the Gouy-Chapman theory assuming a surface charge density of 37 ± 5 Å$^2/e^-$ (Fig. 5), in good agreement with 38 Å$^2/e^-$ found by McLaughlin, Szabo and Eisenman (1971) using similar conditions. A weak binding of Ca^{2+} to the PS bilayer (e.g., McLaughlin *et al.*, 1971; Ohki & Sauve, 1978) cannot be excluded. If this factor is considered, a larger and perhaps more reasonable value for the area per molecule would result (e.g., Papahadjopoulos, 1968). A further factor yielding larger areas per molecule would be a correction for dielectric saturation in the aqueous phase adjacent to the bilayer (Wang & Bruner, 1978).

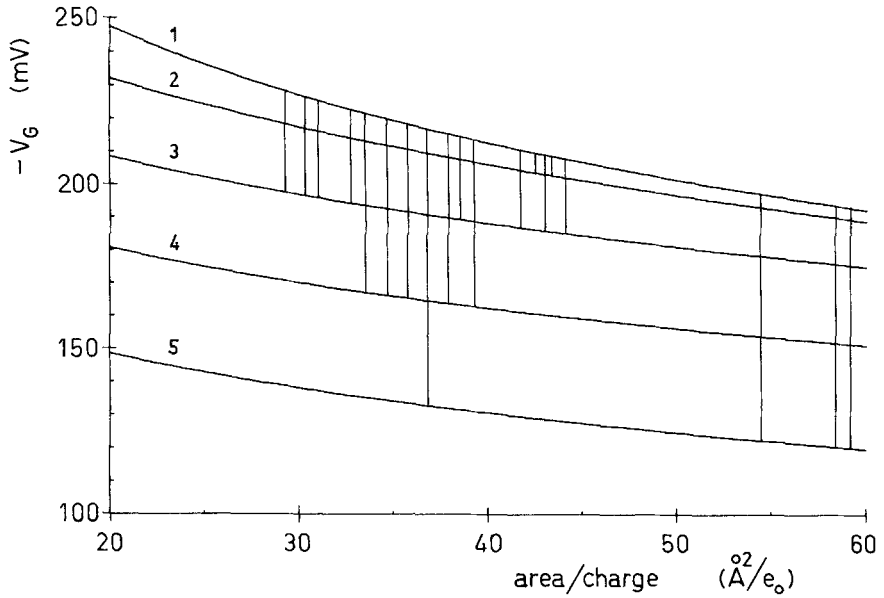

Fig. 5. Determination of the surface charge density by the Gouy-Chapman theory. The curves represent the theoretical surface potential, V_G, as a function of the area/charge, for various electrolyte solutions (*see* below). Calculations for the 2-1-1 electrolytes were done according to Abraham-Schrauner (1975). The experimental values of $V_{C\,\min} = -\Delta V_G$ (vertical bars) were fitted between the curves corresponding to the $CaCl_2$ concentrations on the two sides of the membrane. $CaCl_2$ concentrations are: 0 (curve 1), 10^{-6} M (curve 2), 1.1×10^{-5} M (curve 3), 1.1×10^{-4} M (curve 4), and 1.1×10^{-3} M (curve 5). In all cases 0.011 M 1−1 electrolyte was assumed in accordance with the experimental conditions: 0.01 M KCl, 2 mM imidazole, pH 7.0. Disregarding the 3 values at the far right, the analysis yields a mean area per phosphatidyl serine molecule of 37 ± 5 Å^2

Conclusions

The capacitance minimization method presented in this report for the determination of differences in surface potentials of asymmetric lipid bilayers allows a rapid and simple measurement of dipole and surface charge potentials. Interference by external probes (e.g., carriers) or dependence on a particular analytical model is eliminated.

The results obtained with this simple method are in good agreement with those found by the analysis of current-voltage characteristics and can probably be considered as more reliable. Our results are also consistent with the Gouy-Chapman theory of surface charge potentials, although the exact numerical predictions of this theory may be questionable very near the surface of highly charged membranes.

In many situations the apparatus can be even simpler than that described here: if bilayer conductance is small compared with the capacitive admittance, then one needn't select the 90° current component and can simply use an alternating current amplifier.

In addition to studies of basic bilayer properties, a major application of the technique presented in this paper will be the quantitative measurement of adsorption to lipid membranes of charged, surface active substances, such as membrane active peptides and proteins.

Appendix

The Nernst-Planck Equation Applied to an Asymmetric Trapezoidal Barrier for One Symmetrically Distributed Permeant Species

Essentially we follow the derivations of Neumcke & Läuger (1969) and Hladky (1974). For this reason, only significant modifications based on our explicit allowance of an asymmetric barrier profile will be pointed out.

The trapezoidal potential barrier (Fig. 1*c*) is described by the parameters $\Phi 1(0)$ and $\Phi 2(0)$ (heights of the two corners in mV), d (thickness of the membrane), n (local, dimensionless variable ranging from 0 to 1 across the membrane), and $n1$ and $n2$ (positions of the two corners).

We need an explicit expression only for the portion of the barrier between $n1$ and $n2$. Using the constant field approximation, we can write

$$\Phi 1(V) = \Phi 1(0) + n1 \cdot V$$

and (A1)

$$\Phi 2(V) = \Phi 2(0) + n2 \cdot V.$$

Thus Φ^*, the potential relative to $\Phi 1(V)$, is given by

$$\Phi^*(n, V) = \frac{(\Phi 2(V) - \Phi 1(V))}{n2 - n1} \cdot (n - n1)$$

$$= \frac{(\Delta\Phi + (n2 - n1) \cdot V)}{n2 - n1} \cdot (n - n1) \qquad \text{(A2)}$$

where $\Delta\Phi = \Phi 2(0) - \Phi 1(0)$.

Taking account of the asymmetric barrier shape, the equilibrium concentrations of the permeant complex at the two corners become

$$c(n1, V) = c_i c_s \gamma_s K_a e^{-a(\Phi 1(0) + n1 \cdot V)}$$

and (A3)

$$c(n2, V) = c_i c_s \gamma_s K_a e^{-a(\Phi 2(0) + (n2-1) V)}.$$

Integrating the Nernst-Planck equation between $n1$ and $n2$ and substituting the above concentrations yields

$$I_m = K \frac{(\Delta\Phi + (n2-n1) V)}{n2-n1} \frac{e^{aV} - 1}{e^{a(\Delta\Phi + n2 \cdot V)} - e^{an1 \cdot V}} \tag{A4}$$

with

$$K = \frac{azFAD}{d} c_i c_s \gamma_s K_a \exp(-a\Phi 1(0)). \tag{A5}$$

Symbols

The symbols used are:

I_m – current through the membrane
z – valence of the transported species (=1)
a – $=zF/RT$
A – membrane area
d – membrane thickness
D – intramembranous diffusion coefficient
c_i – bulk concentration of K^+
c_s – bulk concentration of free carrier
γ_s – partition coefficient of the free carrier
K_a – aqueous association constant between K^+ and nonactin

The other symbols have their usual meanings.

References

Abraham-Shrauner, B. 1975. Generalized Gouy-Chapman potential of charged phospholipid membranes with divalent cations. *J. Math. Biol.* **2**:333

Alvarez, O., Latorre, R. 1978. Voltage-dependent capacitance in lipid bilayers made from monolayers. Biophys. J. **21**:1

Aveyard, R., Haydon, D.A. 1973. An Introduction to the Principles of Surface Chemistry. Cambridge University Press, London-New York

Babakov, A.V., Ermishkin, L.N., Liberman, E.A. 1966. Influence of electric field on the capacity of phospholipid membranes. Nature (*London*) **210**:953

Benz, R., Fröhlich, O., Läuger, P., Montal, M. 1975. Electrical capacity of black lipid films and of lipid bilayers made from monolayers. *Biochim. Biophys. Acta* **394**:323

Benz, R., Gisin, B.F. 1978. Influence of membrane structure on ion transport through lipid bilayer membranes. *J. Membrane Biol.* **40**:293

Benz, R., Janko, K. 1976. Voltage-induced capacitance relaxation of lipid bilayer membranes. Effects of membrane composition. *Biochim. Biophys. Acta* **455**:721

Ciani, S.M., Eisenman, G., Laprade, R., Szabo, G. 1973. Theoretical analysis of carrier-mediated electrical properties of bilayer membranes. *In:* Membranes – A Series of Advances. G. Eisenman, editor. Vol. 2, p. 61. Marcel Dekker, New York

Fettiplace, R., Andrews, D.M., Haydon, D.A. 1971. The thickness, composition and structure of some lipid bilayers and natural membranes. *J. Membrane Biol.* **5**:277

Hall, J.E., Latorre, R. 1976. Nonactin-K^+ complex as a probe for membrane asymmetry. *Biophys. J.* **16**:99

Hall, J.E., Mead, C.A., Szabo, G. 1973. A barrier model for current flow in lipid bilayer membranes. *J. Membrane Biol.* **11**:75

Haydon, D.A. 1975. Functions of the lipid in bilayer ion permeability. *Ann. N.Y. Acad. Sci.* **264**:2

Haydon, D.A., Hladky, S.B. 1972. Ion transport across thin lipid membranes: A critical discussion of mechanisms in selected systems. *Q. Rev. Biophys.* **5**:187

Hladky, S.B. 1972. The steady-state theory of the carrier transport of ions. *J. Membrane Biol.* **10**:67

Hladky, S.B. 1973. The effect of stirring on the flux of carriers into black lipid membranes. *Biochim. Biophys. Acta* **307**:261

Hladky, S.B. 1974. The energy barriers to ion transport by nonactin across thin lipid membranes. *Biochim. Biophys. Acta* **352**:71

Hladky, S.B. 1975. Tests of the carrier model for ion transport by nonactin and trinactin. *Biochim. Biophys. Acta* **375**:327

James, F., Roos, M. 1975. Minuit – A system for function minimization and analysis of the parameter errors and correlations. *Comput. Phys. Commun.* **10**:343

Krasne, S., Eisenman, G. 1976. Influence of molecular variations of ionophore and lipid on the selective ion permeability of membranes: I. Tetranactin and the methylation of nonactin-type carriers. *J. Membrane Biol.* **30**:1

Latorre, R., Hall, J.E. 1976. Dipole potential measurements in asymmetric membranes. *Nature (London)* **264**:361

Läuger, P., Neumcke, B. 1973. Theoretical analysis of ion conductance in lipid bilayer membranes. *In:* Membranes – A Series of Advances. G. Eisenman, editor. Vol. 2, p. 1. Marcel Dekker, New York

Läuger, P., Stark, G. 1970. Kinetics of carrier-mediated ion transport across lipid bilayer membranes. *Biochim. Biophys. Acta* **211**:458

McLaughlin, S. 1977. Electrostatic potentials at membrane-solution interfaces. *In:* Current Topics in Membranes and Transport. F. Bronner and A. Kleinzeller, editors. p. 71. Academic Press, New York

McLaughlin, S., Szabo, G., Eisenman, G. 1971. Divalent ions and the surface potential of charged phospholipid membranes. *J. Gen. Physiol.* **58**:667

Montal, M., Mueller, P. 1972. Formation of bimolecular membranes from lipid monolayers and a study of their electrical properties. *Proc. Nat. Acad. Sci. USA* **69**:3561

Neumcke, B., Läuger, P. 1969. Nonlinear electrical effects in lipid bilayer membranes. II. Integration of the generalized Nernst-Planck equations. *Biophys. J.* **9**:1160

Ohki, S., Sauve, R. 1978. Surface potential of phosphatidyl serine monolayers. I. Divalent ion binding effect. *Biochim. Biophys. Acta* **511**:377

Papahadjopoulos, D. 1968. Surface properties of acidic phospholipids: Interaction of monolayers and hydrated liquid crystals with uni- and bi-valent metal ions. *Biochim. Biophys. Acta* **163**:240

Parsegian, V.A. 1975. Ion-membrane interactions as structural forces. *Ann. N.Y. Acad. Sci. USA* **264**:161

Requena, J., Haydon, D.A., Hladky, S.B. 1975. Lenses and the compression of black lipid membranes by an electric field. *Biophys. J.* **15**:77

Schoch, P., Sargent, D.F. 1976. Surface potentials of asymmetric charged lipid bilayers. *Experientia* **32**:811

Stark, G., Benz, R. 1971. The transport of potassium through lipid bilayer membranes by the neutral carriers valinomycin and monactin. *J. Membrane Biol.* **5**:133

Strehlow, H. 1966. Electrode potentials in non-aqueous solvents. *In:* The Chemistry of Non-Aqueous Solvents. J.J. Lagowski, editor. Vol. 1, p. 129. Academic Press, New York

Wang, C.-C., Bruner, L.J. 1978. Dielectric saturation of the aqueous boundary layers adjacent to charged bilayer membranes. *J. Membrane Biol.* **38**:311

White, S.H. 1970. A study of lipid bilayer membrane stability using precise measurements of specific capacitance. *Biophys. J.* **10**:1127

White, S.H., Thompson, T.E. 1973. Capacitance, area, and thickness variations in thin lipid films. *Biochim. Biophys. Acta* **323**:7

Wipf, H.-K., Pioda, L.A.R., Štefanac, Z., Simon, W. 1968. Komplexe von Enniatinen und anderen Antibiotica mit Alkalimetall-Ionen. *Helv. Chim. Acta* **51**:377

Wobschall, D. 1972. Voltage dependence of bilayer membrane capacitance. *J. Colloid Interface Sci.* **40**:417